

RSC Advances



This is an *Accepted Manuscript*, which has been through the Royal Society of Chemistry peer review process and has been accepted for publication.

Accepted Manuscripts are published online shortly after acceptance, before technical editing, formatting and proof reading. Using this free service, authors can make their results available to the community, in citable form, before we publish the edited article. This *Accepted Manuscript* will be replaced by the edited, formatted and paginated article as soon as this is available.

You can find more information about *Accepted Manuscripts* in the [Information for Authors](#).

Please note that technical editing may introduce minor changes to the text and/or graphics, which may alter content. The journal's standard [Terms & Conditions](#) and the [Ethical guidelines](#) still apply. In no event shall the Royal Society of Chemistry be held responsible for any errors or omissions in this *Accepted Manuscript* or any consequences arising from the use of any information it contains.

Raney Nickel-Catalyzed Reductive *N*-methylation of Amines with Paraformaldehyde: Theoretical and Experimental Study

Xin Ge, Chenxi Luo, Chao Qian*, Zhiping Yu, Xinzhi Chen

Key Laboratory of Biomass Chemical Engineering of Ministry of Education, Department of
Chemical and Biological Engineering, Zhejiang University, P.R China

Abstract

Raney Ni-catalyzed reductive *N*-methylation of amines with paraformaldehyde has been investigated. This reaction is proceeded in high yield with water as a byproduct. Raney Ni can be easily recovered and reused with the slight decline of yield. Using the density functional theory (DFT), the mechanism of Raney Ni-catalyzed reductive *N*-methylation are discussed in detail. The reaction pathway undergoes the addition of amine with formaldehyde, dehydration to form the imine and hydrogenation. In the transition state of hemiaminal dehydration, the C-O bond cleavage of aromatic amine is more difficulty than that of aliphatic amine. For aromatic amine, it needs overcoming higher energy barrier, which results in the relatively low yield. After addition of amine with formaldehyde and dehydration, imine is obtained and preferred to adsorb on the bridge site of Ni(111) surface. It is the preferential pathways of imine hydrogenation that the pre-adsorbed hydrogen atom attacks the nitrogen atom of imine. The energy barrier of hydrogenation is much lower than that of addition and dehydration. Thus, the hydrogenation of imine is a relatively rapid reaction step. In the reductive *N*-methylation of secondary amine, the possible dehydration pathway is different from the one of the primary amine. In the dehydration of secondary amine, the intermediate hemiaminal is initially adsorbed on the bridge site of Ni(111) surface, then undergoes C-O bond cleavage, eventually the hydroxyl is located in bridge site. With the final hydrogenation, the product is got by adsorption on the top site of Ni(111) surface.

*Corresponding author. Tel: +86-571-87951615, Fax: +86-571-87951615,

E-Mail: qianchao@zju.edu.cn

Introduction

N-methyl amines are important class of compounds, which play a major role in the synthesis of dyes, surfactants, preservatives, pesticides, herbicides and medicinal intermediates^{1, 2}. *N*-methyl amine is typically synthesized by conventional alkylating agents, such as methyl halide and dimethyl sulfate. However, it has some problems due to the toxic nature of conventional alkylating agents, the poor atom economy and the need of a large number of acid-binding agents³.

For the *N*-alkylation, the reductive alkylation of amine with aldehydes and ketones is an attractive and alternative procedure⁴. It is an efficient protocol to use hydride reducing agents such as sodium borohydride⁵, sodium cyanoborohydride⁶ *etc.* However, this procedure only applies to the laboratory scale due to the high cost of hydride reducing agents. Leuckart-Wallach (LW) reaction is well known, which proceeds condensation of carbonyl with amines to imines and reduction with formic acid as a reducing agent⁷⁻⁹. As the LW reaction suffers from the high temperature (about 180°C), transition metal such as nickel, copper and metal ligand are used to overcome this drawback¹⁰. Although formic acid is clean and high efficient, the atom economy is poor.

Another attractive protocol is the reductive *N*-alkylation of amines with aldehydes and ketones catalyzed by the transition metal, such as Pd, Ni, Pt and so on^{11, 12}. Moreover, these catalysts can be recovered and reused¹³. The mechanism of the transition metal catalyzed reductive *N*-alkylation of amines has long been known that it proceeded addition of aldehydes or ketones with amines, hemiaminal dehydration and imine hydrogenation¹¹. However, the reaction barrier, the mode of adsorption on metal surface and hydrogenation pathways involved in the reductive *N*-alkylation are still unclear. The density functional theory (DFT) calculations can offer a convenient access to study these issues.

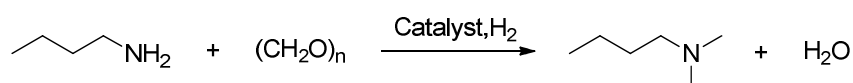
In this paper, we explore Raney Ni-catalyzed reductive *N*-methylation of amines with paraformaldehyde using hydrogen as reductant. The addition, dehydration, adsorption on Ni surface and hydrogenation pathways involved in the reductive *N*-methylation are studied. A detailed investigation on mechanism studies on the Ni surface by using DFT is discussed.

Results and Discussion

As commercial concentrated formaldehyde is a solution of approximately 37% formaldehyde in water with 10-15% methanol, it is not accurate and it is difficult for accurate quantification of formaldehyde. It was reported that the paraformaldehyde could dissociate to formaldehyde by heating¹⁴. Thus, paraformaldehyde was used to study reductive *N*-methylation of amine. Initially, we studied reductive *N*-methylation of *n*-butylamine with paraformaldehyde as the model reaction for screening the transition metal-based catalysts and reaction parameters (Table 1). To our delight, the product was obtained in 93% yield and 100% conversion by using Raney Ni as catalyst at 115 °C under 1.6 Mpa hydrogen gas atmosphere in methanol solvent (Table 1, entry 4). Raney Cu and Co failed to catalyze this reaction in high yield, affording 61% and 48% yield separately (Table 1, entries 2 and 6). When 5 wt.% Pd/C and 5 wt.% Pt/C were used to catalyze this *N*-methylation, the yields were only obtained in 26% and 32% separately (Table 1, entries 3 and 5). Then the catalyst loading and solvent were examined. Firstly, the catalyst loading was investigated (Table 1, entries 4, 7 and 8). As expected, the

lower catalyst loading (2 wt.%) resulted in yield decreasing and the reaction time prolonging. And the higher catalyst loading (8 wt.%) led to the decline of yield. The appropriate Raney Ni loading was 4 wt.%. Secondly, the solvent effect was studied. It was enclosed that methanol was the best solvent (Table 1, entries 4, 9 and 10). To study whether Raney Ni could be recovered and reused, we carried out a recycling test of Raney Ni to catalyze *N*-methylation of *n*-butylamine with paraformaldehyde (in Figure.1). When the reaction completed, Raney Ni was easily recovered by filtration and methanol washing. Subsequently, recovered Raney Ni directly was reused to catalyze this reaction. After four cycles, the slight decline of yield was observed.

Table.1 *N*-methylation of *n*-butylamine with paraformaldehyde^a



Entry	Catalyst (wt.%)	Solvent	Time/h	Cov/%	Yield/% ^b
1	-	Methanol	4	22	0
2	Raney Cu (4)	Methanol	4	80	61
3	Pt/C (5 wt.%) (4)	Methanol	4	57	26
4	Raney Ni (4)	Methanol	4	100	93
5	Pd/C (5 wt.%) (4)	Methanol	4	64	32
6	Co (4)	Methanol	4	67	48
7	Raney Ni (2)	Methanol	6	94	78
8	Raney Ni (8)	Methanol	2	100	82
9	Raney Ni (4)	Water	4	100	87
10	Raney Ni (4)	Hexane	4	79	53

^a Paraformaldehyde (10.496 g, 350 mmol), *n*-butylamine (11.117 g, 152 mmol) and catalyst were added to solvent (100 ml) in a 250 ml autoclave. The mixture was heated to 115 °C

^b Isolated yield.

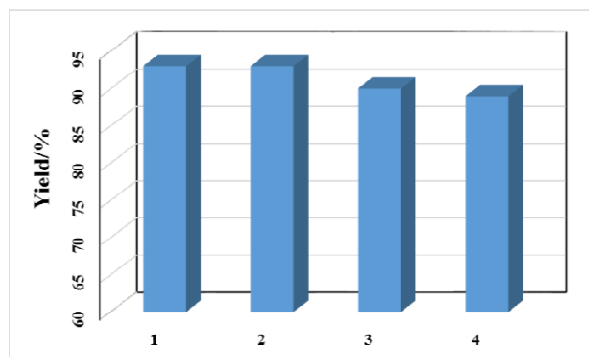
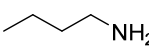
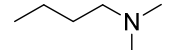
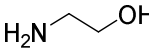
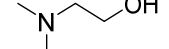
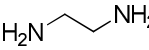
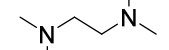
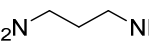
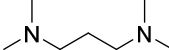
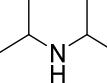
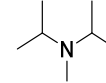
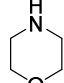
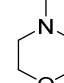
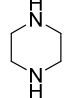
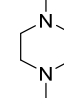
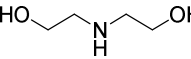
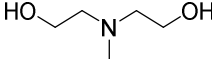


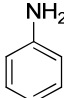
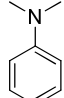
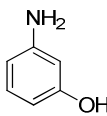
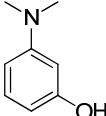
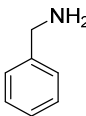
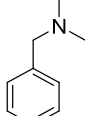
Figure.1 Recycling and reuse of Raney Ni

^a Paraformaldehyde (10.496 g, 350 mmol), *n*-butylamine (11.117 g, 152 mmol) and Raney Ni (445 mg) were added to solvent (100 ml) in a 250 ml autoclave. The mixture was heated to 115 °C

^b Isolated yield.

Table 2. Raney Ni-catalyzed reductive *N*-methylation of amines with paraformaldehyde ^a

Entry	Amine	Product	Raney Ni/wt. %	n(paraformaldehyde): n(amine) ^b	Temperature/°C	Pressure/MPa	Time/h	Yield/% ^c
1			4	2.3	115	1.6	4	93
2			4	2.3	115	1.6	4	90
3			5	4.4	130	2.0	4.5	89
4			5	4.4	130	2.0	4.5	85
5			5	1.2	125	1.4	4	90
6			3	1.05	100	1.3	3	97
7			4	2.1	105	1.5	3.5	95
8			5	1.2	125	1.4	4	92

9			6	2.5	180	1.7	7	65
10			6	2.5	180	1.7	8	21
11			6	2.5	180	1.7	4	80

^a Paraformaldehyde, amine and Raney Ni were added to methanol (100 ml) in a 250 ml autoclave.

^b This ratio refers to formaldehyde equivalents.

^c Isolated yield.

Having identified the Raney Ni could catalyze *N*-methylation of *n*-butylamine with paraformaldehyde, the substrate scope of amines was further explored. In the reductive *N*-methylation of primary amines with paraformaldehyde, the yields were good (85%-93%, Table 2, entries 1-4). The yields of the reductive *N*-methylation of secondary amines were excellent (90-97%, Table 2, entries 5-8). With the steps of *N*-methylation increasing, the reaction course was prolonged and the mono and multi-methyl products couldn't be converted to final product completely. Thus the yield was slightly declining. The aromatic group had adverse effect on the yield (Table 2, entries 9-10). The 80% yield of benzylamine in the reductive *N*-methylation is higher than aniline (Table 2, entry 11). Thus, it is notable that aromatic amine has less activity than aliphatic amine. The possible reasons will be discussed in the following section.

The paraformaldehyde can dissociate to formaldehyde by heating¹⁴. Thus, paraformaldehyde firstly dissociated to formaldehyde and formaldehyde took place this reductive *N*-methylation. The proposed mechanism of Raney Ni-catalyzed reductive *N*-methylation of *n*-butylamine with paraformaldehyde in Figure.2 is proceeded through twice *N*-methylation: the addition of *n*-butylamine with formaldehyde, dehydration to form the imine, enamines, or iminium ions and hydrogenation¹⁵⁻¹⁸. Paraformaldehyde firstly dissociates to formaldehyde. In the *N*-methylation of *n*-butylamine, the second *N*-methylation is slightly different from the first one. As iminium ions **13** are unstable in the alkaline aqueous, the formation of imine in the second *N*-methylation will be studied. So we attempt to find the appropriate reaction pathways of Raney Ni-catalyzed reductive *N*-methylation of *n*-butylamine with paraformaldehyde by the computational study.

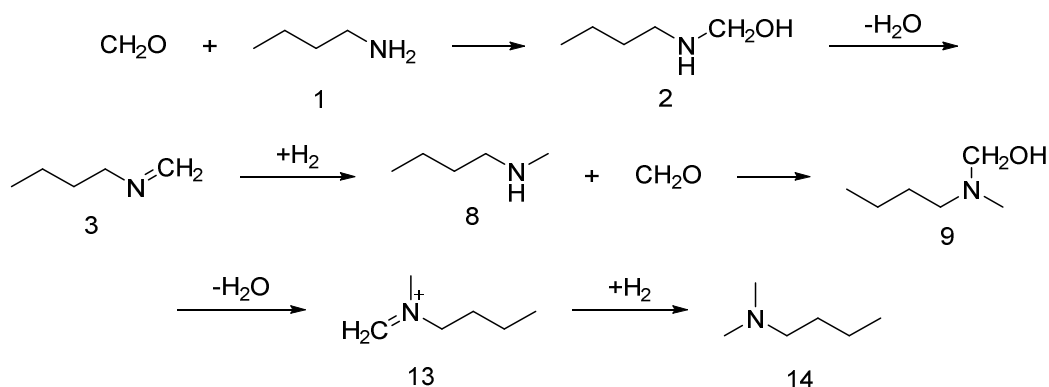


Figure. 2 The proposed mechanism of Raney Ni-catalyzed reductive *N*-methylation of *n*-butylamine with paraformaldehyde

As Figure.3 shown, Raney Ni catalyst has three diffraction peaks of Ni(111), Ni(200) and Ni(220) and Ni(111) is the main diffraction peak. At present, the study on Ni(111) for the chemisorption of CO₂¹⁹⁻²¹, formic acid²⁰⁻²³ and aromatic compounds²⁴⁻²⁹ has gain great achievements. The aromatic ring, formic acid and CO₂ are adsorbed on the Ni(111) surface via the π orbitals or lone electron pair. Imine has similar structure. Moreover, Ni(111) is a well-understanding and convenient model system. Thus, Ni(111) model is used to illuminate the mechanism by the investigation on the formation of imine, adsorption and hydrogenation.

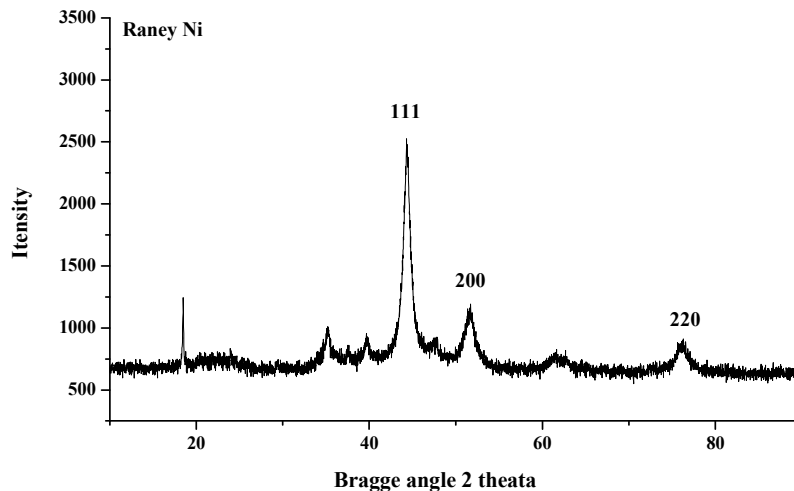


Figure.3 X-ray diffraction patterns of Raney Ni catalyst

Formation of Imine

Formaldehyde can couple with *n*-butylamine **1a** to form hemiaminal **2a** (in Figure.4). The transition state **Ts1a** with 174.8 kJ/mol barrier, describes the mechanism of the addition reaction. With the hydrogen atom of amino group getting close to the carbonyl, the distance between C and H atoms is stretched to 1.313 Å. Simultaneously, the electronegative of N atom and the electropositive of C atom on the carbonyl are gradually strengthened, which promotes the C-N bond formation. Then, the H atom of amino group is transferred to the carbonyl group. Finally, the product hemiaminal **2a** is formed. As strong protic solvent, methanol can improve hydrogen atom transfer capacity in this reaction. The dehydration of hemiaminal **2a** affords the imine **3a**. In the transition state **TS2a**, the hydroxyl group is initially formed by the C-O bond cleavage, and then it localizes the electron density of H atom that the C-H distance is stretched. The break of the C-H bond leads to the formation of imine. The formation of *N*-phenylmethanimine **3b** is similar to **3a**. However, the energy barrier of the transition state **Ts2b** with 263.6 kJ/mol is higher than **Ts2a** with 211.2 kJ/mol. Thus, in transition state **Ts2b**, the cleavage of the C-O bond is more difficulty. It can explicate that the yield of aromatic amine in the reductive *N*-methylation catalyzed by Raney Ni is lower than that of aliphatic amine.

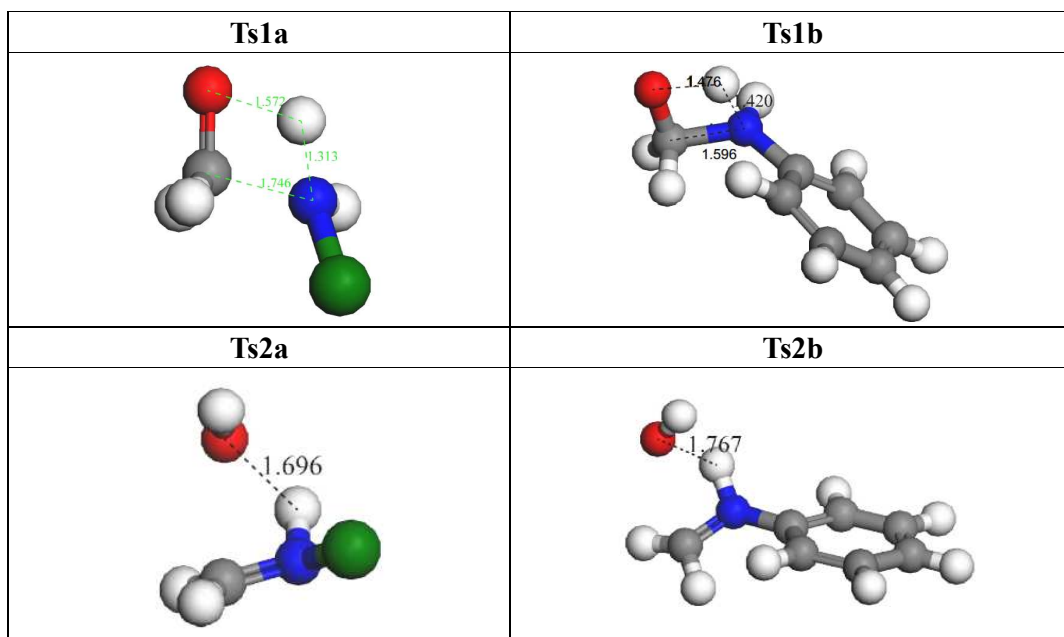
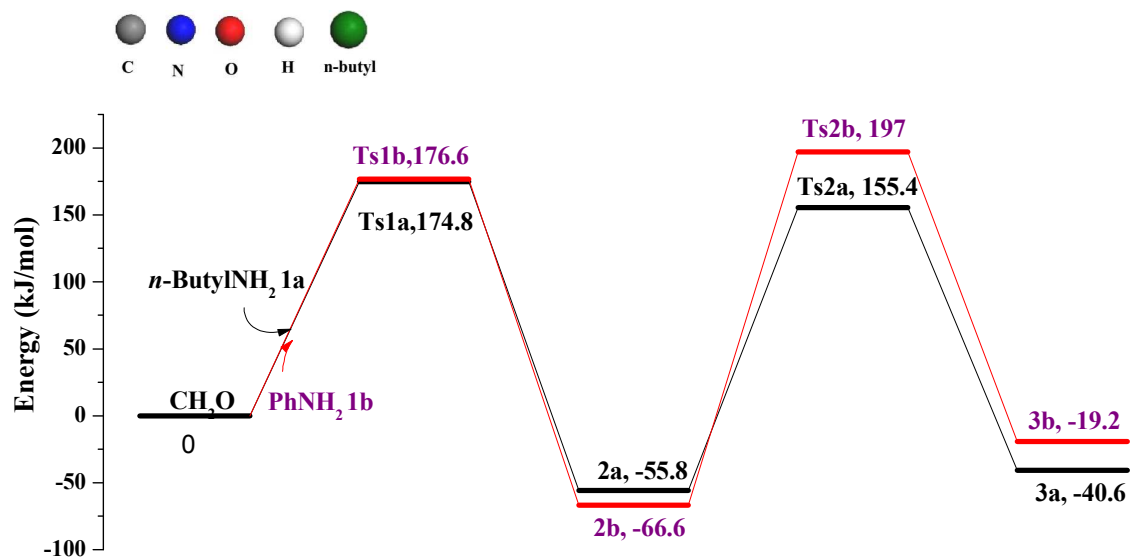


Figure.4 Energy profile of the formation of imine

Adsorption of imine on Ni(111)

As shown in Figure.5, imine can be adsorbed on Ni(111) surface via two adsorption sites, bridge and top. The bridge site with adsorption enthalpy of -153.0 kJ/mol, forms via the C=N double bond cleavage and bonding between C, N atoms and the two neighboring Ni atoms on Ni(111) surface. Two hydrogen atoms, nitrogen atom and Ni atom separately bond with C-centered, forming a tetrahedral. The prolongation of C-N bond from 1.279 Å to 1.371 Å and the configuration change of imine illustrate that the hybrid orbitals of C, N varied from sp^2 to sp^3 . It eventually results in the C=N double

bond cleavage. The distances of C-Ni and N-Ni are 2.064 Å and 1.841 Å, respectively. For top site with calculated adsorption enthalpy of -111.1 kJ/mol, the imine is adsorbed on Ni(111) surface via a N-Ni bond of 2.001 Å. Therefore, the more stable site is the bridge adsorption site.

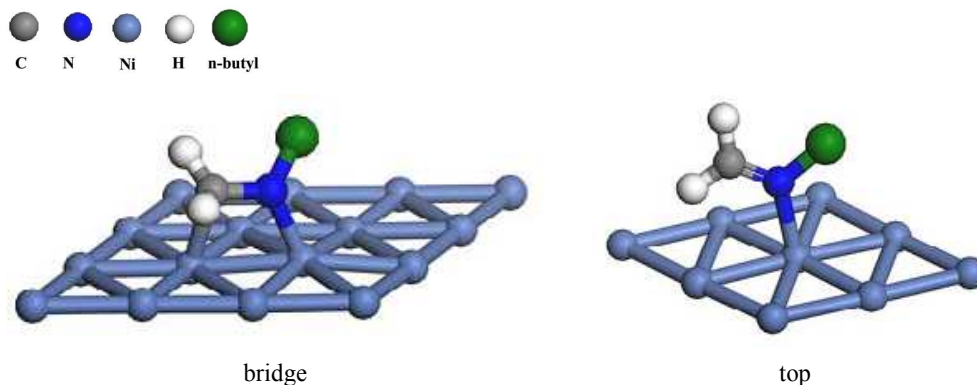


Figure.5 The adsorption site of imine on Ni(111) surface

Hydrogenation of imine

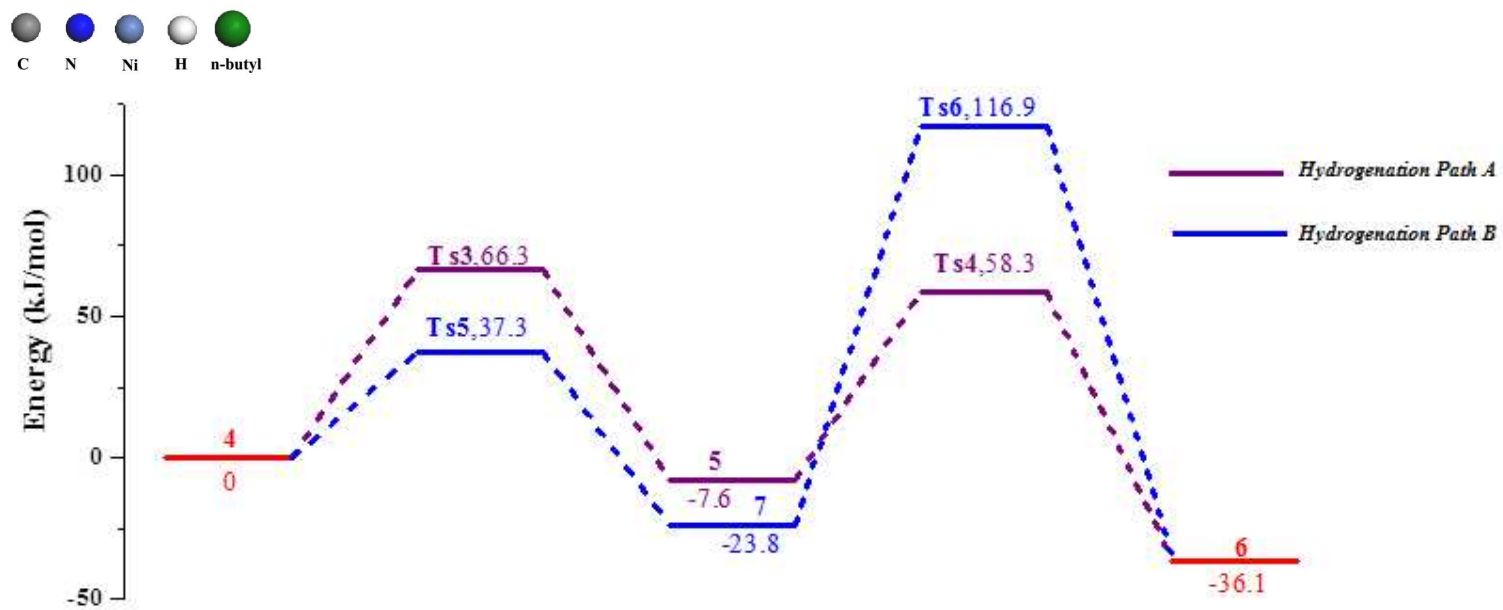
As the bridge adsorption site is the preferred site on Ni(111) surface, we only study the hydrogenation of imine adsorbed in bridge adsorption site. Hydrogenation of imine on Ni(111) surface proceeds two reaction pathways. One of them is that the N atom of imine is firstly attacked by H atom and the C atom from formaldehyde further bonds with another H atom to form *N*-methyl *n*-butylamine **8** (in Figure.6, purple curve, hydrogenation path A). The other reaction pathway is that the C atom from formaldehyde firstly reacts with H atom and then the H atom attacks the N atom (in Figure.6, blue curve, hydrogenation path B). In this reductive *N*-methylation, the hydrogen molecule is initially dissociated to H atom over the top site of on Ni(111) surface without barrier, which is consistent with the reported³⁰. The dissociated H atom has priority for the adsorption on Ni(111) surface via location in the hollow site. In migrate of H atom from the top site to hollow site, there is no energy barrier (see supporting information).

Hydrogenation Path A. On the hydrogen pre-adsorbed Ni(111) surface, the hydrogenation of imine firstly takes place to the N atom with energy barrier of 66.3 kJ/mol. The lone pair electron of N atom involves in bonding. The hydrogenation of N atom gives rise to a slight drift of C-N bond. In the following hydrogenation step, the C atom from formaldehyde reacts with H atom by overcoming an energy barrier of 66.9 kJ/mol. When H atom approaches C atom from formaldehyde, the C-N bond is slightly drifted again. It stretches the C-Ni distance from 1.956 Å to 2.193 Å. Thus, the C-Ni bond is weakened and it eventually leads to C-Ni bond break.

Hydrogenation Path B. After overcoming an energy barrier of 37.3 kJ/mol, the C atom from formaldehyde is hydrogenated. With the C-Ni bond broken, the adsorption site of N atom is transferred from top site to bridge site. As the steric hindrance around the N atom, the H atom approaches the N atom with high energy to cross the 140.7 kJ/mol barrier. In the second hydrogenation step, bridge adsorption site is transferred to top adsorption site again.

In sum, path A is a preferred hydrogenation pathway. It is initiated by N atom attacked by pre-adsorbed H atom and followed by C-H bonding and the C-Ni bond broken. Finally, the imine is hydrogenated to *N*-methyl *n*-butylamine **8** adsorbed on Ni(111) surface via the top site. By comparing **Ts1a**, **Ts2a**, **Ts3** and **Ts4**, the energy barrier of hydrogenation is much lower than addition and dehydration. Therefore, the hydrogenation of imine is relatively rapid reaction step. It is consistent with the reductive

N-methylation of benzaldehyde catalyzed by Pd/C that the imine is hydrogenated very rapidly¹².



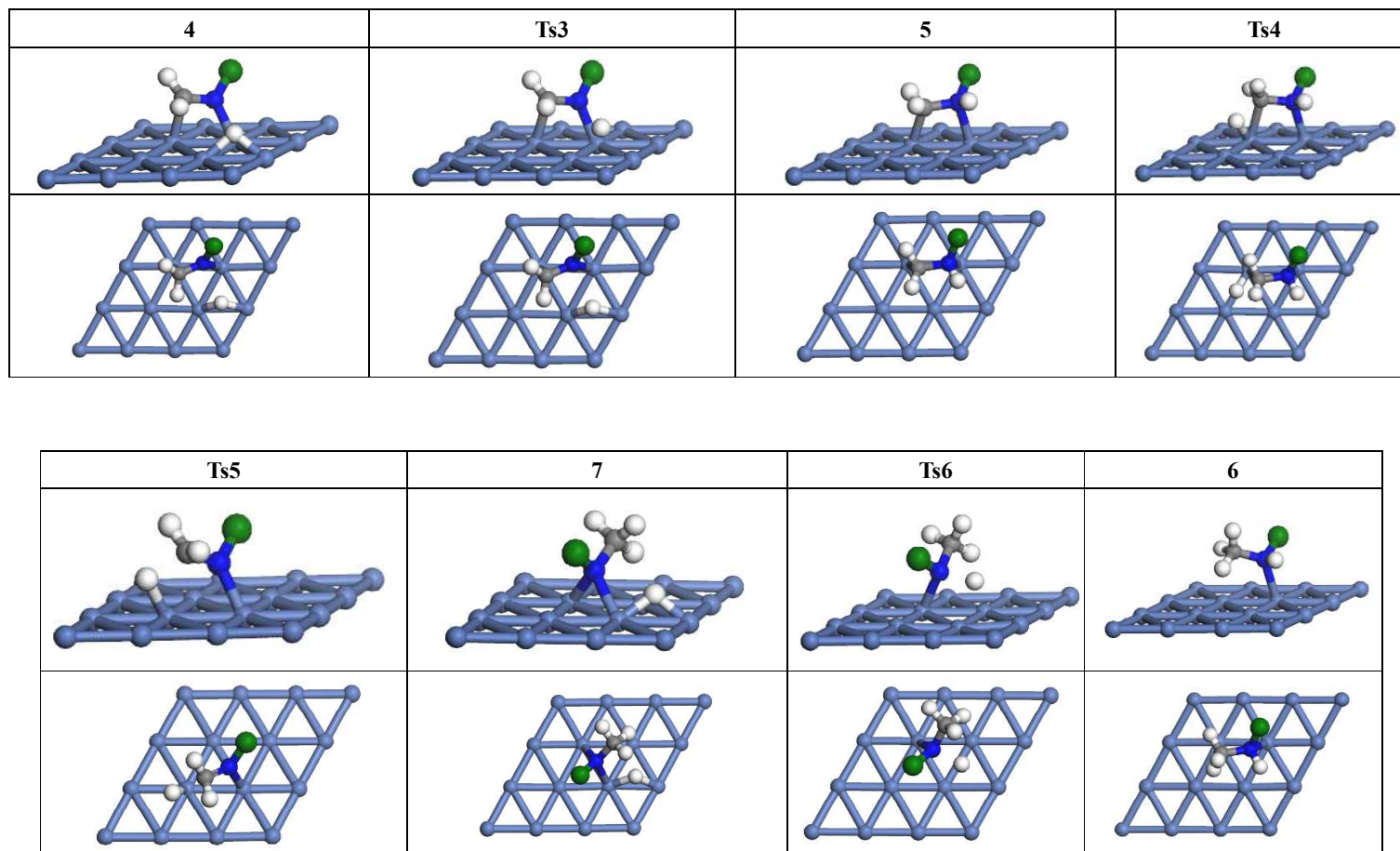


Figure.6 Reaction pathways of imine hydrogenation on Ni(111) surface

Reductive *N*-methylation of secondary amine

As a secondary amine, *N*-methyl *n*-butylamine **8** was obtained. Reductive *N*-methylation of secondary amine is also initiated by addition of amine with formaldehyde. The transition state **Ts7** is similar to **Ts1a** (in Figure.7). When the distance between C and H atoms is stretched to 1.318 Å, the distance between O and H atoms is getting close to 1.543 Å, finally, the C-N bond is formed. Although methyl group increases steric hindrance, the electron-donating ability of methyl group is dominant. Thus, the 139.3 kJ/mol energy barrier of the transition state **Ts7** is lower than **Ts1a**. Similar to hemiaminal **2**, hemiaminal **9** is unstable and can dehydrate. As the iminium ions do not exist in the alkaline aqueous, hemiaminal **9** takes place dehydration by adsorption on Ni(111) surface³¹ (in Figure.8). Firstly, hemiaminal **9** is preferred to adsorb on Ni(111) surface via bridge site. In transition state **Ts8**, the dehydration is initiated by C-O bond cleavage with the energy barrier of 152.6 kJ/mol. The new C-Ni bond is formed by *sp*³ hybrid orbital of C bonding with Ni atom. The adsorption site of the intermediate **11** is still bridge site. The hydroxyl is located in bridge site, which is the preferred adsorption²¹. The following step is the hydrogenation of intermediate **11**. While the H atom is approaching the C atom, the drift of C atom breaks the C-Ni bond. After overcoming the energy barrier of 74.7 kJ/mol, the final product *N,N*-dimethyl butylamine adsorbed on Ni(111) surface via N-Ni sing bond is obtained. The energy barrier of hydrogenation is still much lower than addition and dehydration.

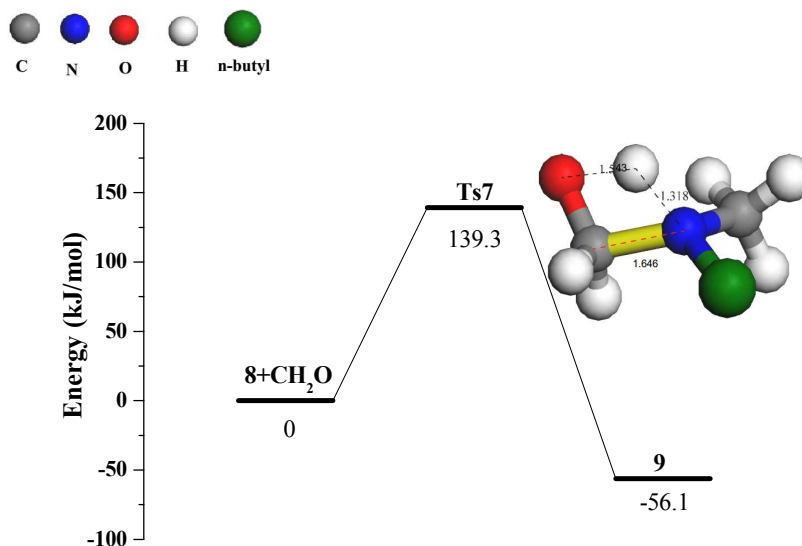


Figure.7 Energy profile of *N*-methyl *n*-butylamine addition

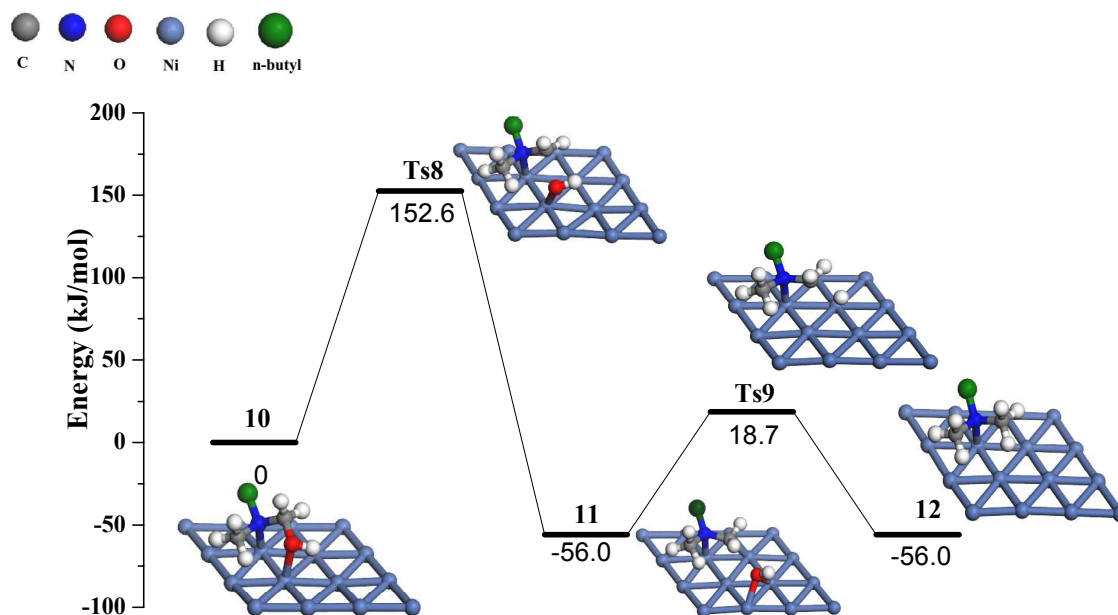


Figure.8 Energy profile of hemiaminal dehydration and hydrogenation on Ni(111) surface

Conclusion

In sum, the reductive *N*-methylation of amines with paraformaldehyde catalyzed by Raney Ni is described. The reductive *N*-methylation proceeds in high yield through the addition of amine with formaldehyde, and the dehydration to form the imine and hydrogenation, which is investigated by DFT. Raney Ni can be recovered and reused with the slight decrease of yield after four cycles. In the transition state of hemiaminal dehydration, the energy barrier of aromatic amine is higher than the one of aliphatic amine. For aromatic amine, it leads to more difficult cleavage of the C-O bond. Thus, compared with aliphatic amine, the yield of aromatic amine is lower in the reductive *N*-methylation catalyzed by Raney Ni. After the condensation of amines with paraformaldehyde, the imine is preferred to adsorb on the bridge site of Ni(111) surface. The imine hydrogenation pathways are discussed in detail. The results show that the nitrogen atom of imine is preferentially attacked by pre-adsorbed hydrogen atom. The energy barrier of hydrogenation is much lower than that of addition and dehydration. The hydrogenation of imine is a relatively rapid reaction step. In the reductive *N*-methylation of secondary amine, the dehydration is slightly different from the previous. The intermediate hemiaminal is preferred to adsorb on the bridge site of Ni(111) surface. The dehydration is initiated by C-O bond cleavage and the hydroxyl is located in bridge site. With the final hydrogenation, the product adsorbed on Ni(111) surface via N-Ni sing bond is obtained.

Experimental Section

Nuclear magnetic resonance (NMR) spectra were measured at 400 MHz (^1H) or at 100 MHz (^{13}C) on a Bruker Avance DRX-400 spectrometer. GC analyses were performed on GC Agilent 1790F series and GC-MS analyses were performed on GC-MS Agilent 5973-6890 series (FID detector, weakly polar capillary column SE-30, nitrogen as carrier gas). The operating parameters of chromatography are as follows: nitrogen 0.1 Mpa, hydrogen 0.1 Mpa, air 0.03 MPa, vaporizing chamber 260 °C and detector 280 °C. The column temperature was carried out by program controlled that initial temperature 60 °C, heating rate 20 °C/min, final temperature 260 °C. XRD analyze was performed on X'Pert PRO. The Raney Ni and Raney Cu were purchased from Zhejiang Metallurgical Research Institute Co., Ltd. All reagents and solvents were general reagent grade. All reactions were carried out in 250 ml autoclave Parr 4576 series.

General procedure for Raney Ni-catalyzed reductive *N*-methylation of amines with paraformaldehyde by using hydrogen as reductant. The synthesis of *N,N*-dimethyl-*n*-butyl amine was selected as model reaction. Paraformaldehyde (10.496 g, 350 mmol), *n*-butylamine (11.117 g, 152 mmol) and Raney Ni (445 mg) were added to methanol (100 ml) in a 250 ml autoclave. The autoclave was purged with nitrogen gas three times and then was purged with hydrogen gas three times, then maintained 1.6 Mpa pressure. The mixture was heated to 115 °C and the pressure was maintained 2.1 Mpa. Then stirring was maintained for 4 h. The pressure was declined to 1.75 Mpa. Raney Ni was recovered by filtration and washed by methanol. Then the reaction mixture was distilled to separate and recover methanol and light component and the product *N,N*-dimethyl-*n*-butylamine was obtained in 93% yield.

***N,N*-dimethyl-*n*-butylamine.** Yield 93%. ^1H NMR (400 MHz, CDCl_3) δ 2.31 – 2.12 (m, 8H), 1.52 – 1.38 (m, 2H), 1.32 (dq, $J = 14.3, 7.1$ Hz, 2H), 0.92 (t, $J = 7.3$ Hz, 3H). ^{13}C NMR (100 MHz, CDCl_3) δ 59.62, 45.48, 29.90, 20.61, 14.01. MS (EI, 70eV), m/z (rel abundance): 101(M^+ , 8), 86(5), 58(100), 44(13), 39(18), 30(88).

***N,N*-dimethyl-2-hydroxyethylamine.** Yield 90%. ^1H NMR (400 MHz, CDCl_3) δ 4.00 (s, 1H), 3.54 (dd, $J = 10.2, 5.0$ Hz, 2H), 2.38 (dd, $J = 10.6, 5.3$ Hz, 2H), 2.18 (d, $J = 5.3$ Hz, 6H). ^{13}C NMR (100 MHz, CDCl_3) δ 61.16, 58.81, 45.25. MS (EI, 70eV), m/z (rel abundance): 89(M^+ , 8), 58(100), 42(31), 30(15).

***N,N,N',N'*-tetramethylethylenediamine.** Yield 89%. ^1H NMR (400 MHz, CDCl_3) δ 2.39 (s, 4H), 2.24 (s, 12H). ^{13}C NMR (100 MHz, CDCl_3) δ 57.58, 45.78. MS (EI, 70eV), m/z (rel abundance): 114(M^+ , 99), 99(11), 71(65), 56(32), 43(100), 28(17).

***N,N,N',N'*-tetramethylpropanediamine.** Yield 85%. ^1H NMR (400 MHz, CDCl_3) δ 2.33 – 2.25 (m, 4H), 2.22 (s, 12H), 1.70 – 1.57 (m, 2H). ^{13}C NMR (100 MHz, CDCl_3) δ 57.80, 45.43, 25.94. MS (EI, 70eV), m/z (rel abundance): 130(M^+ , 5), 85(79), 70(52), 58(100), 42(49), 30(11).

***N,N*-diisopropylmethylamine.** Yield 90%. ^1H NMR (400 MHz, CDCl_3) δ 2.91 (dt, $J = 12.5, 6.2$ Hz, 2H), 2.49 (s, 3 H), 1.04 (d, $J = 6.3$ Hz, 12H). ^{13}C NMR (100 MHz, CDCl_3) δ 59.68, 35.07, 23.30. MS (EI, 70eV), m/z (rel abundance): 115(M^+ , 33), 100(96), 72(18), 58(100), 42(22), 30(13)

***N*-methylmorpholine.** Yield 97%. ^1H NMR (400 MHz, CDCl_3) δ 3.79 – 3.59 (m, 4H), 2.41 (s, 4H), 2.29 (s, 3H). ^{13}C NMR (100 MHz, CDCl_3) δ 66.87, 55.39, 46.40. MS (EI, 70eV), m/z (rel abundance): 101(M^+ , 48), 71(31), 56(6), 43(100), 29(15)

1, 4-dimethylpiperazine. Yield 95%. ^1H NMR (400 MHz, CDCl_3) δ 2.45 (s, 8H), 2.29 (s, 6H). ^{13}C NMR (100 MHz, CDCl_3) δ 55.03, 45.95. MS (EI, 70eV), m/z (rel abundance): 114(M^+ , 99), 99(11),

71(65), 56(32), 43(100), 28(17).

***N*-methyl-diethanolamine.** Yield 92%. ^1H NMR (400 MHz, CDCl_3) δ 4.50 (s, 2H), 3.76 – 3.49 (m, 4H), 2.64 – 2.38 (m, 4H), 2.29 (s, 3H). ^{13}C NMR (100 MHz, CDCl_3) δ 59.51, 58.92, 42.09. MS (EI, 70eV), m/z (rel abundance): 119(M^+ , 3), 88(100), 58(12), 44(91), 31(20).

***N*, *N*-dimethylaniline.** Yield 65%. ^1H NMR (400 MHz, CDCl_3) δ 7.35 – 7.14 (m, 2H), 6.72 (dd, J = 13.2, 7.6 Hz, 3H), 2.93 (s, 6H). ^{13}C NMR (100 MHz, CDCl_3) δ 150.72, 129.09, 116.68, 112.71, 40.64. MS (EI, 70eV), m/z (rel abundance): 120(M^+ , 100), 104(18), 91(7), 77(30), 51(14), 42(9).

3-dimethylamino-phenol. Yield 21%. ^1H NMR (400 MHz, CDCl_3) δ 7.07 (t, J = 8.3 Hz, 1H), 6.37 – 6.29 (m, 1H), 6.24 – 6.17 (m, 2H), 2.88 (s, 6H). ^{13}C NMR (100 MHz, CDCl_3) δ 156.67, 152.22, 130.01, 105.68, 104.12, 100.17, 40.72. MS (EI, 70eV), m/z (rel abundance): 136(M^+ , 100), 121(15), 108(9), 94(13), 65(14), 39(7).

***N*, *N*-dimethyl-1-phenylmethanamine.** Yield 80%. ^1H NMR (400 MHz, CDCl_3) δ 7.36 – 7.27 (m, 4H), 7.27 – 7.18 (m, 1H), 3.41 (s, 2H), 2.23 (s, 6H). ^{13}C NMR (100 MHz, CDCl_3) δ 138.88, 129.13, 128.25, 127.05, 64.44, 45.38. MS (EI, 70eV), m/z (rel abundance): 135(M^+ , 77), 118(9), 91(80), 77(7), 65(25), 58(100), 51(10), 42(25), 30(3).

Computational Details

DFT calculations were carried out by using the CASTEP program package in Materials Studio of Accelrys Inc³²⁻³⁴, where the Perdew, Burke, Erzenhof gradient corrected functional (GGA-PBE) is chosen together with Plane wave basis functions with spin polarization³⁵⁻³⁸. The linear and quadratic synchronoustransit (LST/QST) complete search was chose to search for transition state of the reaction³⁹. The simulation of core electron was performed by Ultrasoft pseudopotential (USP)⁴⁰. In order to improve computational performance, energy cut-off was set 400.0 eV.

Ni(111) surface was modeled by using a three-layer periodic slab model with a (5×5) super cell. Then by building a 10 Å vacuum slab, the adsorption and reaction occurs in this cell. The reciprocal space of the (5×5) super cell was sampled using the 3×3×1 k-points grid. Larger k-points sets were needed if more accurate energy value wanted. Study in this work focused on the relative results of different systems, so the k-points set of (3×3×1) should be enough. For the geometry optimization, all Ni atoms were constrained except the uppermost layer, with setting the convergence tolerances of energy and displacement to 2×10^{-5} eV/atom and 2×10^{-3} Å, respectively, and setting the SCF tolerance to 2×10^{-6} eV/atom.

Chemisorption energies were calculated using the following formulas:

$$\Delta E_{ads} = E_{adsorbate-Ni} - E_{adsorbate} - E_{Ni}$$

Where ΔE_{ads} represented the adsorption energy of the adsorbate on Ni(111) surface, $E_{adsorbate}$ was the energy of free adsorbate, E_N was the energy of clean slab and $E_{adsorbate-Ni}$ was the energy of adsorbate-Ni adsorption system.

For a reaction, such as $A + B \rightarrow C + D$, the energy barrier was calculated as follows:

$$\Delta E_{React} = E_{Ts} - E_{A+B-Ni}$$

Where E_{Ts} is the energy of the transition state and E_{A+B-Ni} is the energy of A+B-Ni adsorption system.

Acknowledgement

The authors are grateful for the financial support from the Natural Science Foundation of China (21376213), the Research Fund for the Doctoral Program of Higher Education of China (20120101110062) and the Low Carbon Fatty Amine Engineering Research Center of Zhejiang Province (2012E10033). Shang Zhicai group is thanked for helping us with calculations.

Reference

1. A. Ricci, *Modern Amination Methods*, Wiley-VCH, New York, 2000.
2. D. A. Horton, G. T. Bourne and M. L. Smythe, *Chem Rev*, 2003, **103**, 893-930.
3. B. S. Michael, *March's Advanced Organic Chemistry: Reactions, Mechanisms, and Structure, 7th Edition*, Wiley, New York, 2013.
4. B. Fu, N. Li, X. M. Liang, T. H. Dong and D. Q. Wang, *Chinese J Org Chem*, 2007, **27**, 1-7.
5. B. Miriyala, S. Bhattacharyya and J. S. Williamson, *Tetrahedron*, 2004, **60**, 1463-1471.
6. R. A. Stalker, T. E. Munsch, J. D. Tran, X. P. Nie, R. Warmuth, A. Beatty and C. B. Aakeroy, *Tetrahedron*, 2002, **58**, 4837-4849.
7. P. L. Debenneville and J. H. Macartney, *J Am Chem Soc*, 1950, **72**, 3073-3075.
8. W. L. Borkowski and E. C. Wagner, *J Org Chem*, 1952, **17**, 1128-1140.
9. K. Ito, H. Oba and M. Sekiya, *B Chem Soc Jpn*, 1976, **49**, 2485-2490.
10. M. Kitamura, D. Lee, S. Hayashi, S. Tanaka and M. Yoshimura, *J Org Chem*, 2002, **67**, 8685-8687.
11. S. Nishimura, *Handbook of Heterogeneous Catalytic Hydrogenation for Organic Synthesis*, Wiley, New York, 2001.
12. A. W. Heinen, J. A. Peters and H. van Bekkum, *Eur J Org Chem*, 2000, 2501-2506.
13. A. Corma and H. Garcia, *Chem Rev*, 2003, **103**, 4307-4365.
14. K. G. Helander, *Biotech Histochem*, 2000, **75**, 19-22.
15. G. E. Dobreiner and R. H. Crabtree, *Chem Rev*, 2010, **110**, 681-703.
16. H. X. Li, X. T. Wang, M. W. Wen and Z. X. Wang, *Eur J Inorg Chem*, 2012, 5011-5020.
17. H. X. Li, X. T. Wang, F. Huang, G. Lu, J. L. Jiang and Z. X. Wang, *Organometallics*, 2011, **30**, 5233-5247.
18. G. Guillena, D. J. Ramon and M. Yus, *Chem Rev*, 2010, **110**, 1611-1641.
19. D. B. Cao, Y. W. Li, J. G. Wang and H. J. Jiao, *J Phys Chem C*, 2011, **115**, 225-233.
20. G. W. Peng, S. J. Sibener, G. C. Schatz, S. T. Ceyer and M. Mavrikakis, *J Phys Chem C*, 2012, **116**, 3001-3006.
21. R. G. Zhang, H. Y. Liu, B. J. Wang and L. X. Ling, *J Phys Chem C*, 2012, **116**, 22266-22280.
22. S. D. Zhou, C. Qian and X. Z. Chen, *Catal. Lett.*, 2011, **141**, 726-734.

23. Q. Q. Luo, G. Feng, M. Beller and H. J. Jiao, *J Phys Chem C*, 2012, **116**, 4149-4156.
24. S. Lehwald, H. Ibach and J. E. Demuth, *Surf Sci*, 1978, **78**, 577-590.
25. Z. Jing and J. L. Whitten, *Surf Sci*, 1991, **250**, 147-158.
26. S. M. Kane, T. S. Rufael, J. L. Gland, D. R. Huntley and D. A. Fischer, *J Phys Chem B*, 1997, **101**, 8486-8491.
27. S. Yamagishi, S. J. Jenkins and D. A. King, *J Chem Phys*, 2001, **114**, 5765-5773.
28. F. Mittendorfer and J. Hafner, *J Phys Chem B*, 2002, **106**, 13299-13305.
29. L. M. Ghiringhelli, R. Caputo and L. Delle Site, *Phys Rev B*, 2007, **75**.
30. G. Kresse, *Phys Rev B*, 2000, **62**, 8295-8305.
31. X. Ge, J. B. Pan, C. Qian, L. Feng, Y. B. Chen and X. Z. Chen, *Catal Commun*, 2014, **46**, 201-207.
32. M. Marlo and V. Milman, *Phys Rev B*, 2000, **62**, 2899-2907.
33. M. C. Payne, M. P. Teter, D. C. Allan, T. A. Arias and J. D. Joannopoulos, *Rev Mod Phys*, 1992, **64**, 1045-1097.
34. G. P. Srivastava and D. Weaire, *Advances in Physics*, 1987, **36**, 463-517.
35. R. A. Vansanten and M. Neurock, *Catal Rev*, 1995, **37**, 557-698.
36. B. Delley, *J Chem Phys*, 2000, **113**, 7756-7764.
37. A. Gil, A. Clotet, J. M. Ricart, G. Kresse, M. Garcia-Hernandez, N. Rosch and P. Sautet, *Surf Sci*, 2003, **530**, 71-86.
38. M. Gajdos, A. Eichler and J. Hafner, *Journal of Physics-Condensed Matter*, 2004, **16**, 1141-1164.
39. J. P. Perdew, K. Burke and M. Ernzerhof, *Phys Rev Lett*, 1996, **77**, 3865-3868.
40. T. A. Halgren and W. N. Lipscomb, *Chem Phys Lett*, 1977, **49**, 225-232.